TECHNICAL REPORT ARCCB-TR-91032

ABSENCE OF EXTERNAL ELECTRIC-FIELD EFFECTS ON TRANSFORMATIONS IN STEELS

P. J. COTE
L. V. MEISEL
T. HICKEY

OCTOBER 1991

US ARMY ARMAMENT RESEARCH,
DEVELOPMENT AND ENGINEERING CENTER
CLOSE COMBAT ARMAMENTS CENTER
BENÉT LABORATORIES
WATERVLIET, N.Y. 12189-4050

APPROVED FOR PUBLIC RELEASE; DISTRIBUTION UNLIMITED

DISCLAIMER

The findings in this report are not to be construed as an official Department of the Army position unless so designated by other authorized documents.

The use of trade name(s) and/or manufacturer(s) does not constitute an official indorsement or approval.

DESTRUCTION NOTICE

For classified documents, follow the procedures in DoD 5200.22-M, Industrial Security Manual, Section II-19 or DoD 5200.1-R, Information Security Program Regulation, Chapter IX.

For unclassified, limited documents, destroy by any method that will prevent disclosure of contents or reconstruction of the document.

For unclassified, unlimited documents, destroy when the report is no longer needed. Do not return it to the originator.

REPORT DOCUMENTATION PAGE

Form Approved
OMB No. 0704-0188

1. AGENCY USE ONLY (Leave blank)	2. REPORT DATE	3. REPORT TYPE AND DATES COVERED
	October 1991	Final

4. TITLE AND SUBTITLE
ABSENCE OF EXTERNAL ELECTRIC-FIELD EFFECTS ON TRANSFORMATIONS IN STEELS

5. FUNDING NUMBERS
AMCMS No. 6111.02.H610.011
PRON No. 1A05Z0CANMSC

6. AUTHOR(S)
P.J. Cote, L.V. Meisel, and T. Hickey

7. PERFORMING ORGANIZATION NAME(S) AND ADDRESS(ES)
U.S. Army ARDEC
Benet Laboratories, SMCAR-CCB-TL
Watervliet, NY 12189-4050

8. PERFORMING ORGANIZATION REPORT NUMBER
ARCCB-TR-91032

9. SPONSORING/MONITORING AGENCY NAME(S) AND ADDRESS(ES)
U.S. Army ARDEC
Close Combat Armaments Center
Picatinny Arsenal, NJ 07806-5000

10. SPONSORING/MONITORING AGENCY REPORT NUMBER

11. SUPPLEMENTARY NOTES
Submitted to Journal of Materials Science.

12a. DISTRIBUTION/AVAILABILITY STATEMENT
Approved for public release; distribution unlimited.

12b. DISTRIBUTION CODE

13. ABSTRACT (Maximum 200 words)

Large hardness increases were recently reported for an ASTM A723 and an O_2 tool steel when a 1 kV/cm external electric (E)-field was applied during the post-austenitization quench. The increased hardness was attributed to a field-induced order of magnitude decrease in the austenite decomposition rate during the quench. The results of an extensive study of austenite decomposition kinetics in the same A723 steel and a similar O_2 tool steel in the presence and absence of E-fields with magnitudes up to 3 kV/cm during post-austenitization cooling are reported here. Differential thermal analysis and thermomagnetic analysis were employed to directly monitor the austenite decomposition processes in both steels. Supplementary hardness measurements in the tool steel are also reported. No effects of external E-fields on austenite transformations were detected.

14. SUBJECT TERMS	15. NUMBER OF PAGES
Electric Field Effects, Steel, Phase Transformations, Thermal Analysis	23
	16. PRICE CODE

17. SECURITY CLASSIFICATION OF REPORT	18. SECURITY CLASSIFICATION OF THIS PAGE	19. SECURITY CLASSIFICATION OF ABSTRACT	20. LIMITATION OF ABSTRACT
UNCLASSIFIED	UNCLASSIFIED	UNCLASSIFIED	UL

TABLE OF CONTENTS

TABLES

LIST OF ILLUSTRATIONS

Page

ACKNOWLEDGEMENTS

We appreciate the assistance of Mr. Christopher Rickard who performed the hardness measurements and the metallography. We thank Mr. Paul Croteau for his assistance in specimen preparation and Mr. Julius Frankel for his critical reading of this manuscript.

INTRODUCTION

Cao et al. (ref 1) recently reported remarkable hardness increases in steel specimens resulting from the application of external electric (E)-fields during heat treatment. They found hardness increased as much as a factor of two within the bulk of quenched, 1.6 to 3-mm diameter specimens when an E-field of 1 kV/cm is applied between the sample and a pair of parallel plates during the quench. They observed a small additional hardness increase when the field is also applied during austenitization. Cao et al. attributed the hardness increases to a field-induced order of magnitude reduction in austenite decomposition rates (i.e., increased hardenability) during quenching.

An O_2 tool steel and a 4340-type steel are discussed in Reference 1. Larger hardness increases were reported for the O_2 tool steel and were explained as a consequence of the higher inherent hardenability of 4340. More detailed studies of the tool steel were published in the proceedings of a recent Army Research Office Workshop on Field Effects on Materials (ref 2).

The work reported here principally employed differential thermal analysis (DTA) and thermomagnetic analysis (TMA) to quantitatively test the conclusions of Cao et al. regarding external E-field effects on transformation rates. DTA and TMA offer the advantage of in-situ monitoring of phase transformations as a given specimen is cycled with and without an externally applied E-field, thereby eliminating effects of variations among samples. Since the major E-field effect is reported on austenite decomposition rates during cooling, this is emphasized: however, results on the influence of E-fields on the austenite transformation on heating are also included. Hardness measurements, which supplement the transformation data, are also presented for the O_2 tool steel.

Specimen and E-field configurations similar to those used by Cao et al. were investigated for both types of steel. No E-field effects on the austenite transformations of the O_2 tool steel or the 4340-type steel could be detected. Thus, the explanation for the E-field effects reported in Reference 1 must be sought elsewhere.

EXPERIMENTAL PROCEDURE

The thermal analysis data were obtained using a modified Mettler TA1 Thermal Analyzer which provides simultaneous digital recordings of DTA and thermogravimetric (TGA) signals. Alumina sample holders of 9-mm diameter were used for sample and reference purposes. High purity copper rods of the same dimensions as the specimen were used as references.

Helmholtz coils were placed around the furnace so that the TGA system emulated a TMA. The coils produced a uniform and a gradient magnetic field which yielded a force on a magnetic specimen that was registered as an apparent change in sample weight. The austenite transformations in these steels were accompanied by changes in magnetic state, so TMA data complemented the DTA data in the present study. Reaction rates were thus determined by thermal means (austenite transformation exotherms) and by magnetization changes (paramagnetic austenite-to-ferromagnetic bainite and paramagnetic austenite-to-ferromagnetic pearlite/ferrite).

The system was also modified to produce an E-field configuration similar to that of Cao et al. (ref 1) within the smaller sample space of the DTA apparatus. Platinum electrodes (5 by 20 mm) served as the negative parallel plates and were held inside the sample holder at an approximate 7-mm separation with a mica insert. A platinum connector for the positive lead was spot-welded directly to

the 3-mm specimens that were positioned midway between the plates. With the 2-mm gap between the specimen and each of the two negative plates, 600 volts produced a mean field of roughly 3 kV/cm in the gap region. This compares with the Cao et al. gap field given as 1 kV/cm with larger (25 by 10 cm) parallel plates maintained at a 2-cm separation. Typical currents ranged from 60 microamps at the 830°C austenitization temperature to 20 microamps or less during the cooling of the sample.

Specimen protection against decarburization was usually provided with a helium 10 percent H_2 gas mixture. Additional protection against decarburization was obtained by copper plating (~ 2 mils) of the steel samples. Plated and unplated samples were used in the present experiments. The specimens were in the form of rods 3-mm in diameter and 19-mm long. The rods used by Cao et al. ranged from 1.6 to 3-mm in thickness and were 25 to 45-mm in length.

The 4340-type steel used by Cao et al. was supplied by the current authors. Material from the same block was used in this study. It is more properly designated as an ASTM A723 steel which is essentially a 4340 steel, refined by electroslag remelting and modified by the addition of 0.1 percent vanadium and with 3.18 percent nickel rather than 1.8 percent nickel assumed by Cao et al. The ASTM designation is used in the remainder of this report. The O_2 tool steel samples were obtained from standard machine shop stock. The compositions of the steels are given in Table I.

TABLE I. STEEL COMPOSITIONS (Weight Percent)

Element	ASTM A723	O_2 Steel
Carbon	0.34	0.88
Manganese	0.62	1.4
Silicon	0.16	0.45
Nickel	3.18	0.03
Chromium	1.02	-
Molybdenum	0.48	0.18
Vanadium	0.10	0.08
Phosphorous	0.008	0.009
Sulfur	0.004	0.003
Aluminum	0.005	-
Tungsten	-	0.10
Cobalt	-	0.28

RESULTS AND DISCUSSION

Transformation-Time Path

The thermal cycles employed for the steels were selected to provide the clearest demonstration possible of E-field effects on the austenite transformations during cooling, while accommodating the large differences in the transformation rates (hardenability) of the two steels and the cooling rate limitations of the apparatus.

The hardenability is sufficiently high in the ASTM A723 steel that a full isothermal transformation at the bainite transformation region (i.e., below the

bainite start temperature (B_S) and above the martensite start temperature (M_S)) can be obtained after cooling from the austenitizing temperature at 20°C/min. Thus, the entire bainite transformation at a given temperature can be monitored in our apparatus.

The high hardenability is demonstrated in Figure 1, which shows DTA and TMA data obtained by cooling ASTM A723 steel from the austenitization temperature at only 10°C/min. The thermal and magnetic data show the classic martensite transformation beginning at M_S, which is approximately 280°C, with no transformation in the bainite region above M_S. Figure 2 shows the corresponding path on the continuous-cooling-transformation (CCT) diagram obtained by examining transformations in a 3.0 weight percent (wt.%) nickel specimen at various cooling rates.

Since the much higher austenite decomposition rates (lower hardenability) and instrumentation limitations precluded the use of isothermal transformations for studies of possible E-field effects in the O_2 tool steel, several convenient continuous cooling paths through the pearlite/ferrite and bainite transformation zones on the CCT diagram (data obtained from Reference 1), illustrated in Figure 3, were chosen.

ASTM A723 Steel

The following thermal cycles were used for the ASTM A723 steel:

1. Heat to an austenitization temperature (837°C) at 25°C/min.
2. Hold for 15 minutes at 837°C.
3. Cool to the selected temperature, in the bainite region, at 25°C/min.
4. Hold (isothermal) at the selected temperature for one hour.

Figures 4 and 5 show the bainite transformation data under E-field-on and E-field-off conditions for a coated specimen during isothermal annealing at 355°C. The data were obtained in consecutive runs on "as-received" material.

The E-field-on preceded the E-field-off case. The reaction rate peaks (the DTA peaks) are slightly different: the E-field-off peak occurs at a slightly longer time and has reduced height indicating a more sluggish bainite transformation for the field-off run. The magnetization data (TMA) reflect the same effect with the magnetization increasing at a slower rate for the field-off case. Essentially the same small changes are obtained for subsequent cycles with no E-fields. Thus, Figures 4 and 5 demonstrate the effect of prior heat treatment; they do not indicate a marginally poorer hardenability for the E-field-on case. The E-field-on first pair is shown to preclude the possibility that prior heat treatment vitiates the E-field effects. Had there been an order of magnitude shift in hardenability with the E-field as concluded by Cao et al. (ref 1), the peak position would be shifted an order of magnitude in time.

An uncoated sample of ASTM A723 was also tested to allay concerns that copper coatihg might interfere with the E-field effect. The results are presented in Figure 6. The isothermal hold temperature was 337°C in this case. The smaller amplitude of the field-off run in this case is due to a combination of the thermal cycling effect and the premature transformation of a small amount of austenite to bainite in the outermost decarburized layers of the specimen prior to initiation of the isothermal hold. As in the coated case, the peak maxima occur at approximately the same time. Thus, no difference between the field-on and field-off cases is observed. (Obviously, no order of magnitude shift can be supported.)

O_2 Tool Steel

The results of the continuous cooling experiments following a 15-minute austenitization at 837°C on O_2 tool steel are given in Figures 7 and 8. The cooling paths of 15°C/min and 50°C/min are shown in Figure 3. The austenite-to-

pearlite/ferrite and austenite-to-bainite transformations are manifested by distinct DTA peaks. The relative quantities of pearlite/ferrite and bainite can be deduced from the relative areas under the peaks. Here, the slower cooling rate of Figure 7 is seen to yield a preponderance of pearlite, while the faster rate of Figure 8 yields a more equal mix of the two austenite decomposition products.

The close similarity of the E-field-on and E-field-off cases at both cooling rates demonstrates the absence of E-field effects on austenite transformations. Furthermore, the large difference in transformation response at the two rates demonstrates the sensitivity of the present experiments to changes in transformation kinetics.

Hardness measurements on O_2 tool steel cooled under E-field-on and E-field-off conditions at a cooling rate of 50°C/min are in complete accord with the transformation data cited above. The Knoop hardnesses (deduced from 20 points along the length of sectioned specimens) were identical (425 ± 1 Kg/mm²) for E-field-on and off.

Cao et al. (ref 3) also concluded that the transformation to austenite, which occurs on heating, is significantly accelerated by the application of an external field. We examined this transformation for numerous heating runs on both ASTM A723 and O_2 tool steel and found no evidence of an E-field effect. Figure 9 shows the typical null result we obtained.

Comments on the Cao et al. Procedures and Results

The reported order of magnitude increase in steel hardenability with an external E-field is difficult to understand. The main explanations suggested by Cao et al. (ref 1) require E-fields within the bulk of the metal. In the experiments of Cao et al., the sample is the center positive electrode separated

from two negative plates by an insulating medium (air/oil). Cao et al. measure an electric current of 200 microamps, which flows through the quenching media (silicone and mineral oil) during the quench where the major field effect occurs, implying that E ≈ 10^{-9} volts/cm within the metal. The size of the current is many orders of magnitude less than any previously reported (ref 2) to produce significant effects on material properties. Thus, it would seem that an alternative explanation of their effects is needed.

There is a serious problem with the quench procedure employed for the O_2 tool steel in Reference 1. The treatment, which yields the largest E-field effect, involves a quench into silicone oil maintained at 145°C. As indicated in Figure 3, this is at or above M_S for O_2 tool steel, which means that their process is actually an interrupted quench with an isothermal hold in the lower bainite region. The amount of bainite formed in such a thermal process depends on the hold time, which is not given; if the hold time were not controlled, such a procedure would produce large variations in properties from one run to another because the properties of lower bainite differ substantially from the untempered martensite produced in a complete quench.

A further complication is that lower bainite is often difficult to distinguish from martensite, which may explain why Cao et al. report that martensite is the main constituent in a procedure that is commonly used to produce bainite.

The E-field-off results for the quench into silicone oil maintained at 145°C are also perplexing. Cao et al. report that a cooling rate of 20°C/sec produces a predominately pearlitic microstructure in their O_2 specimen. The CCT diagram indicates that only a small amount of pearlite will form at this high

rate. Our data in Figures 7 and 8 are in accord with the CCT diagram and indicate that a reduction of several orders of magnitude in cooling rate (from 20°C/sec) is required to yield a predominately pearlitic microstructure. We suggest that the key question in this regard concerns the unusual softness (300 to 400 VHN) of the E-field-off cases and not the high hardnesses (800 to 900 VHN) of the E-field-on cases, since such high hardnesses are the rule with oil quenching of small specimens of tool steel.

Another mystery is their observation of bainite in 2 by 3-mm rod specimens of ASTM A723 at the cooling rates of their experiments: At cooling rates of approximately 30°C/sec, bainite is reported to form without the E-field, while no bainite forms when the E-field is applied. They also observe bainite after air quenches, for which the quench rate is given as approximately 5°C/sec. The problem here is that the hardenability of this steel is much too high to form appreciable amounts of bainite at these cooling rates in the absence of E-fields. The 3.18 percent nickel in this steel produces an order of magnitude shift in the bainite knee to longer times relative to 4340 steels. The data in our Figure 1 show that cooling this steel at 10°C/min (i.e., 0.17°C/sec) is sufficient to bypass the bainite knee. Therefore, the possibility of bainite in oil-quenched 2 by 3-mm rods of this ASTM A723 steel is essentially precluded.

In addition to the improper quench procedure, a factor in their surprising findings may be the lack of any specimen protection during heat treatments. Their experiments were conducted in air where oxidation and decarburization at high temperatures (up to 870°C in their experiments) are rapid and will significantly alter the chemistry of thin samples. (We observed serious decarburization and oxidation when we tried experiments in air.) An assessment of

the surface condition of their specimens might provide a clue as to the source of the reported phenomenon.

CONCLUSIONS

The present work establishes that external E-fields of magnitude as large as 3 kV/cm produce essentially no changes in austenite transformation kinetics for the same 4340-type steel (ASTM A723) studied by Cao et al. (ref 1) or for an O_2 tool steel, similar to that studied by Cao et al. Furthermore, in the present work, hardness values measured for O_2 tool steels quenched with and without E-fields are indistinguishable.

The present results refute the hypothesis that external E-fields produce order of magnitude reductions of austenite decomposition rates in ASTM A723 and O_2 tool steels. The present study also reveals problems in the experimental procedures of Cao et al. (refs 1,2) which may either be responsible for these mysterious observations or may be obscuring their origins.

REFERENCES

1. W. D. Cao, X. P. Lu, A. F. Sprecher, and H. Conrad. Materials Letters, Vol. 9, 1990, p. 193.

2. H. Conrad and I. Ahmad (eds.), Proceedings of the U.S. Army Workshop on High Intensity Electromagnetic and Ultrasonic Effects on Inorganic Materials Behavior and Processing, North Carolina State University, Raleigh, NC, July 1989.

3. H. Conrad, Private Communication, North Carolina State University, Raleigh, NC, 1990.

Note Added in Proof: We have recently been informed through internal ARO reports that Cao et al. now believe that the specimen which they labeled as O_2 tool steel contains less than half the amount of managanese of commerical O_2 tool steel. This only minimally affects the contents of this report, since the hypothesis in question is implied to be a universal phenomenon.

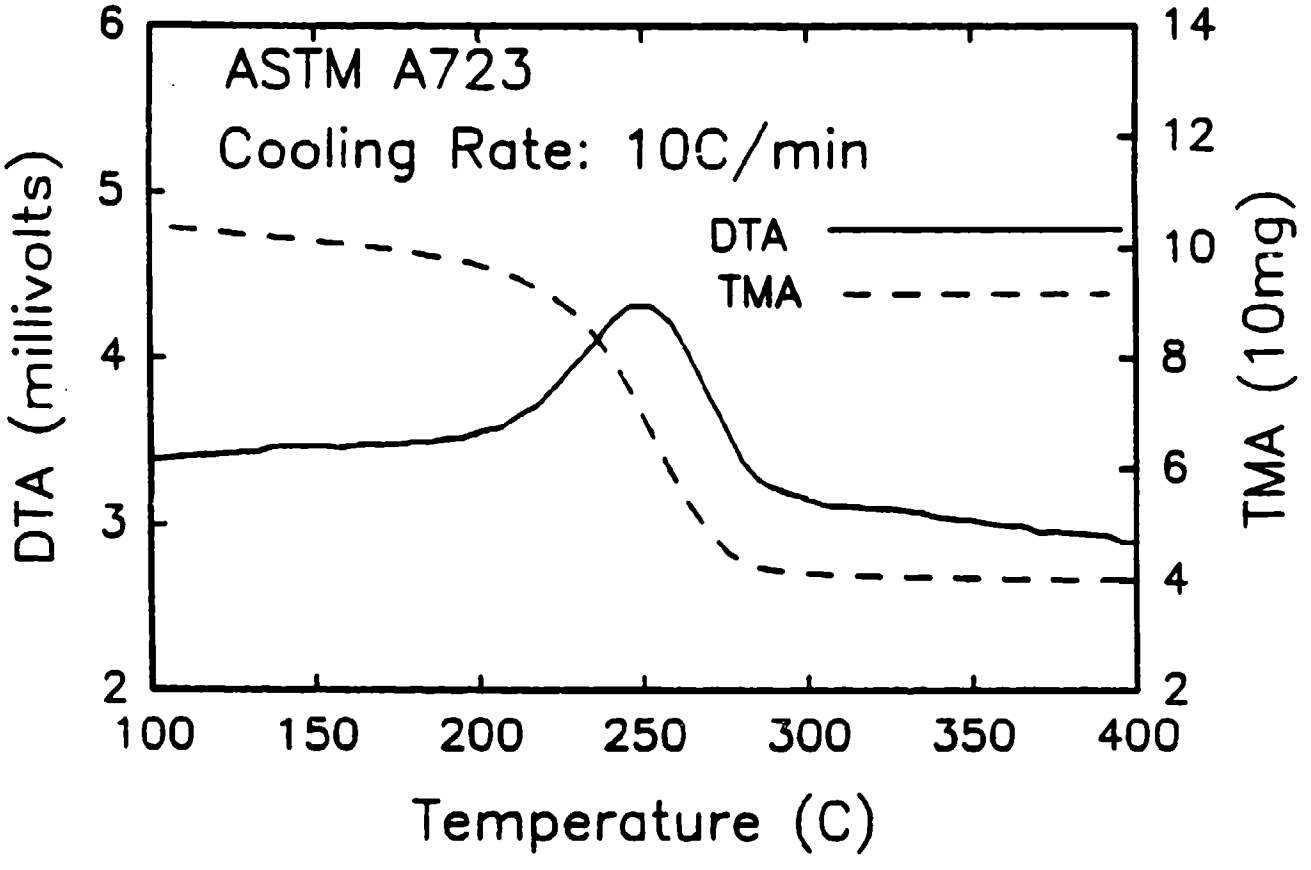

Figure 1. DTA and TMA data illustrating high hardenability of the 3.18 percent nickel composition ASTM A723. Both measurements show the martensite transformation beginning at about 280°C with no detectable bainite. In this case, the zero magnetic force corresponds to four units on the TMA axis. The magnetic force increases monotonically with an amount of (ferromagnetic) martensite transformed from (paramagnetic) austenite.

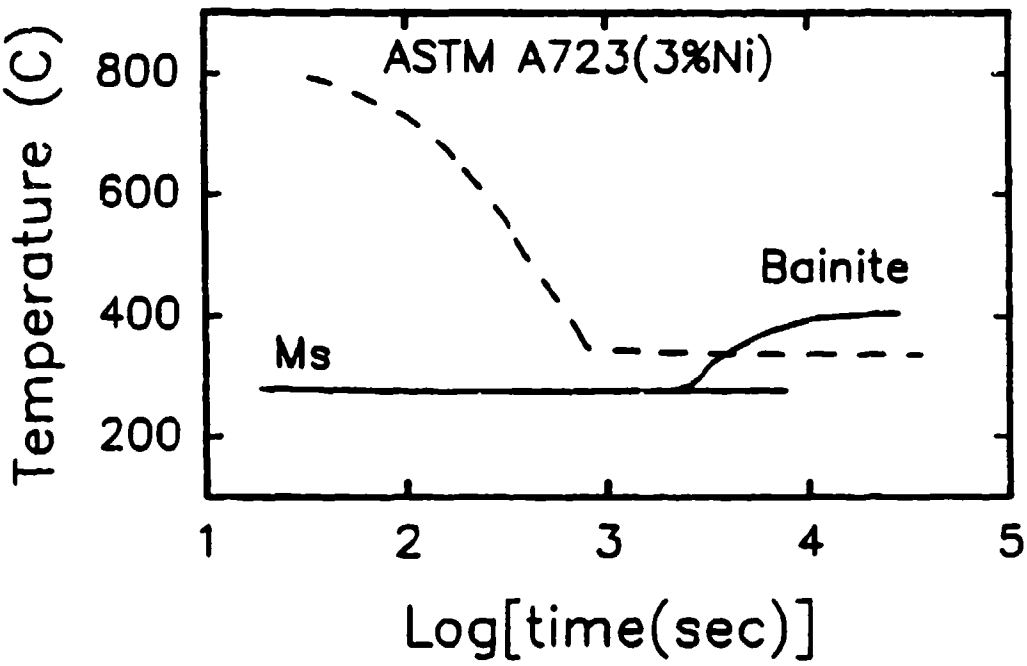

Figure 2. Approximate CCT diagram for the high nickel composition used in the present measurements. The dashed line shows the cooling path used in the isothermal studies of the bainite transformation.

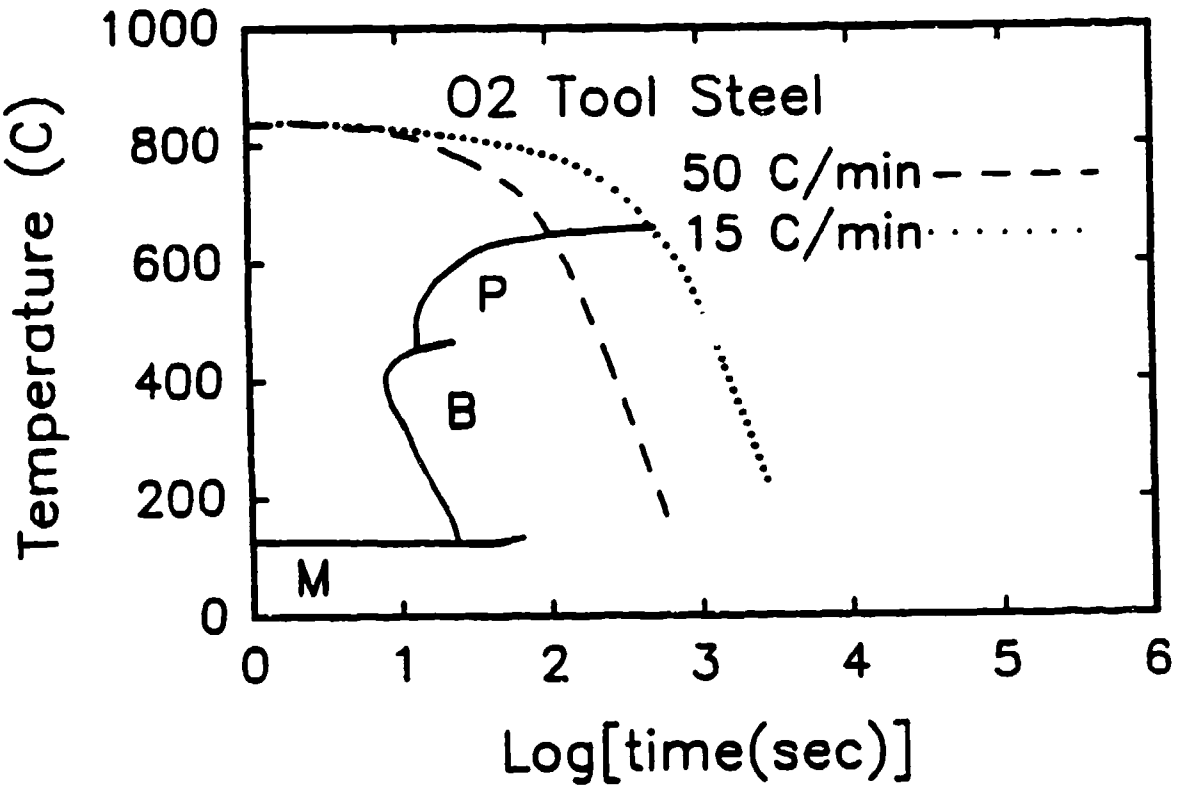

Figure 3. Main features of CCT diagram for O_2 tool steel. Dashed lines show cooling paths used in the present E-field effect studies.

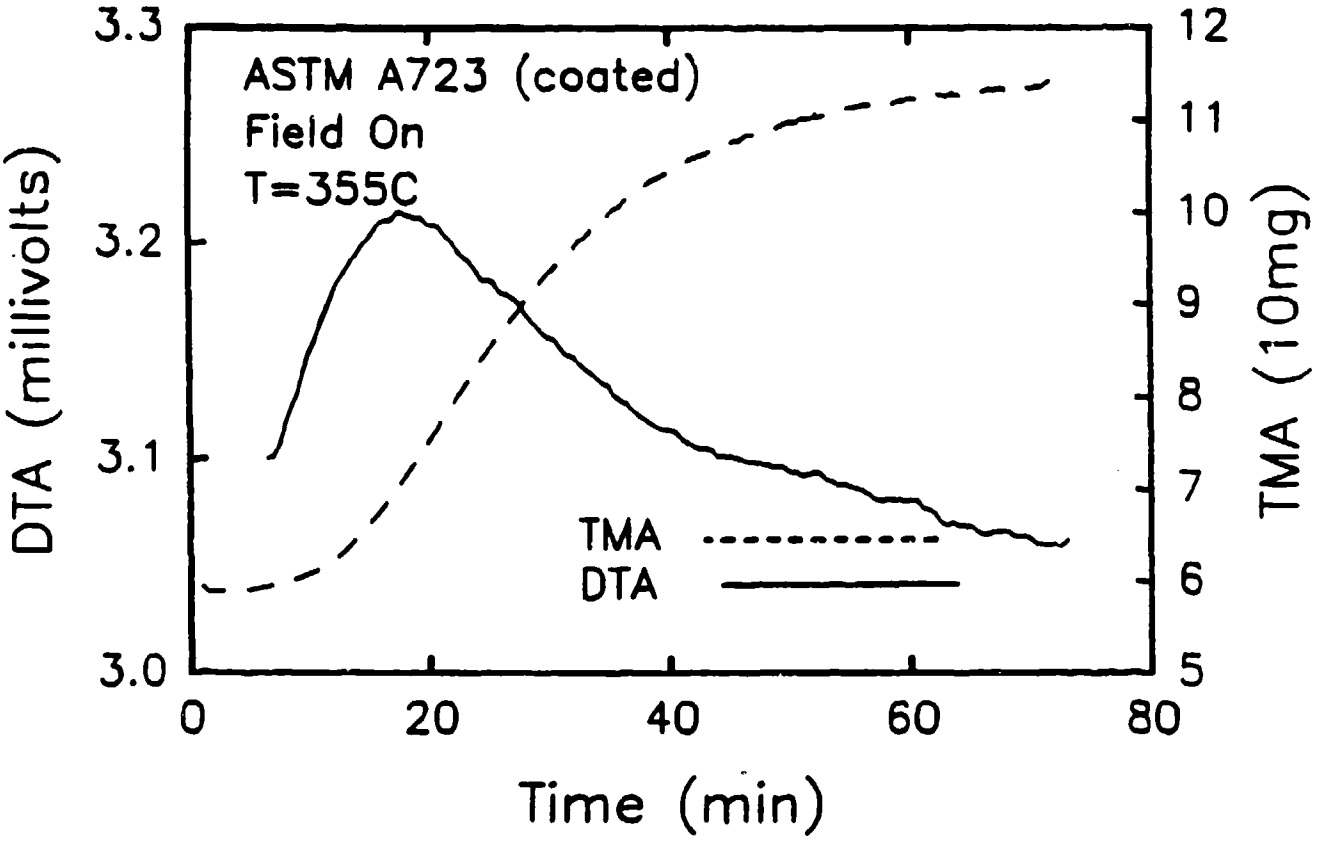

Figure 4. DTA and TMA data for the 355°C isothermal bainite transformation with an applied external E-field of 3 kV/cm. As the transformation progresses from austenite (paramagnetic) to bainite (ferromagnetic), the magnetic force increases from zero (~ 6 TMA units) to its full value (~ 11.5 TMA units). The specimen was copper plated.

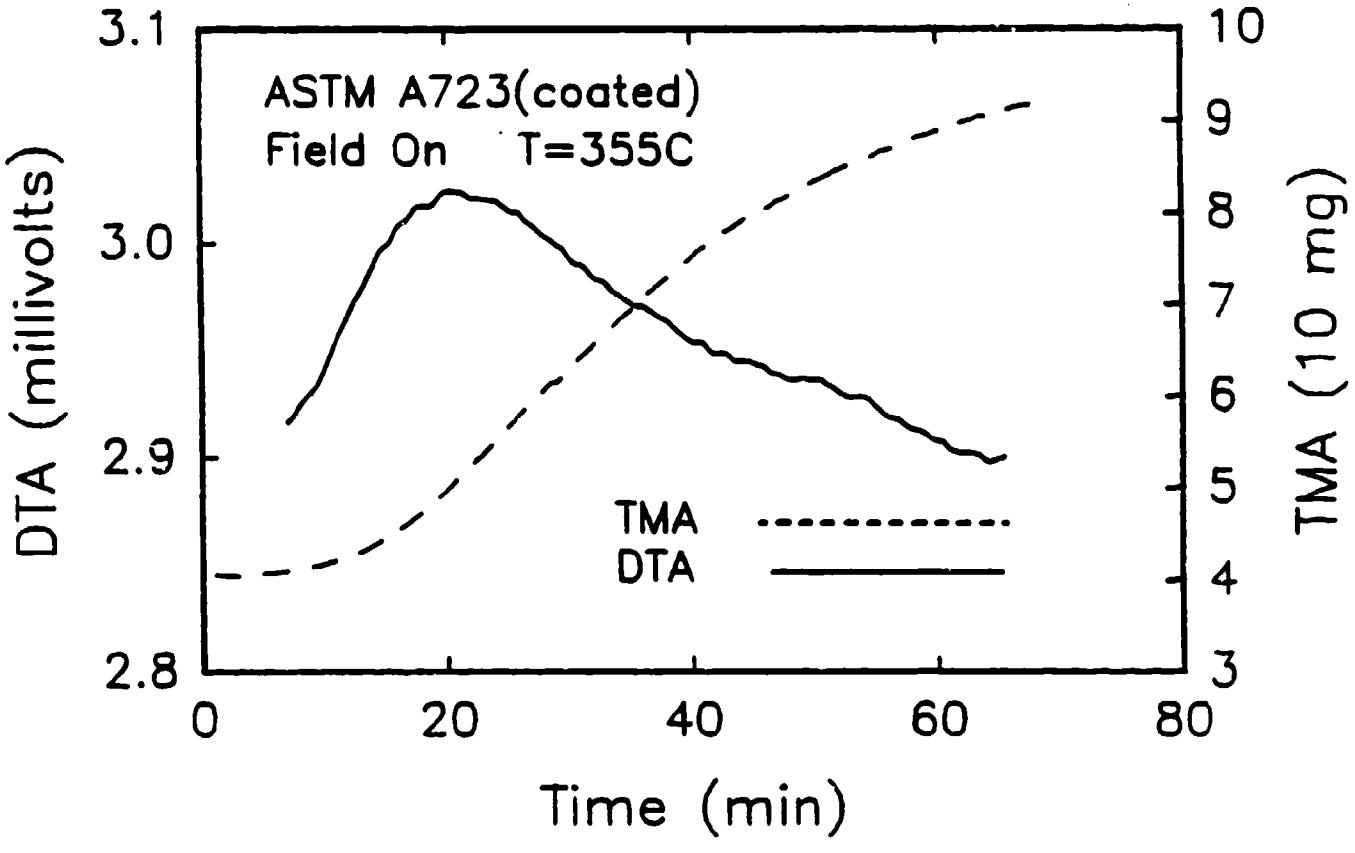

Figure 5. DTA and TMA data for the 355°C isothermal bainite transformation with no applied E-field. The magnetic force varies from zero (~ 4 TMA units) to its full value (~ 9.5 TMA units) as the transformation progresses from (paramagnetic) austenite to (ferromagnetic) bainite. The specimen was copper plated.

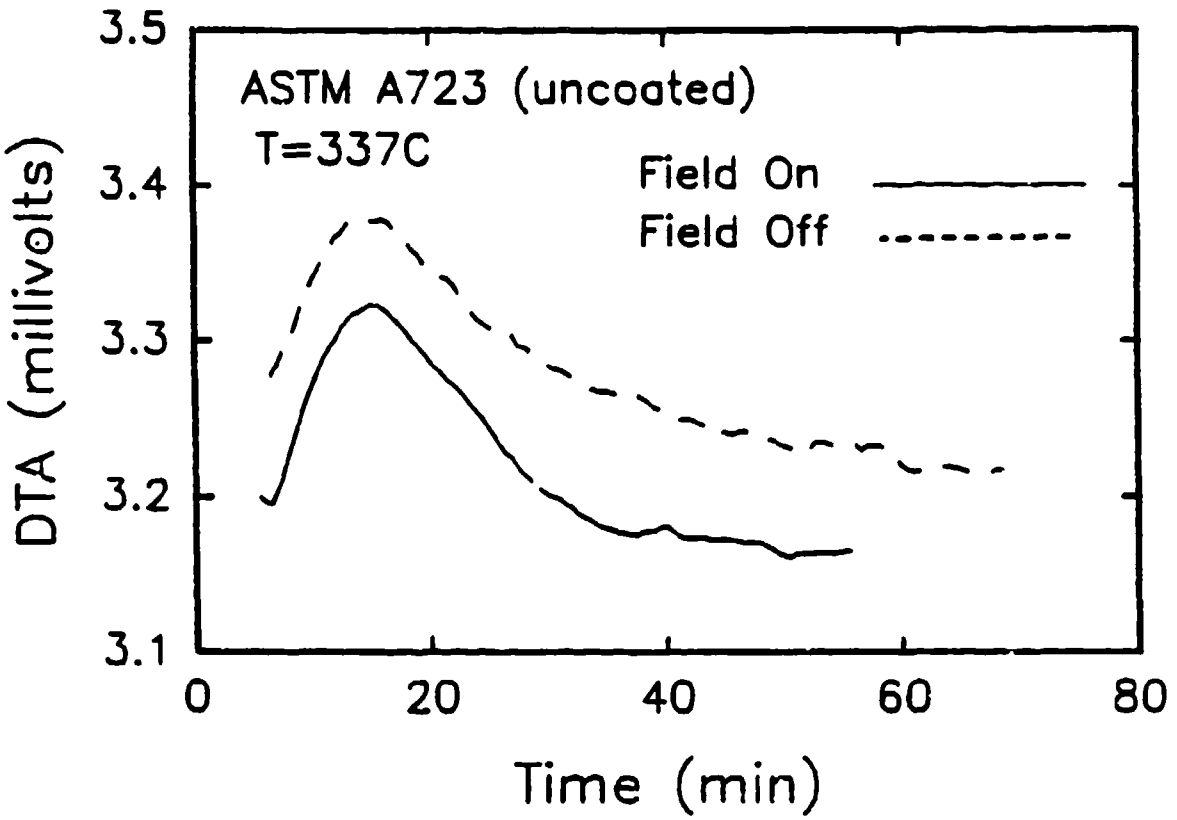

Figure 6. DTA output for the isothermal transformation of bainite in ASTM A723 at 337°C using an uncoated specimen under E-field-on (3 kV/cm) and E-field-off conditions.

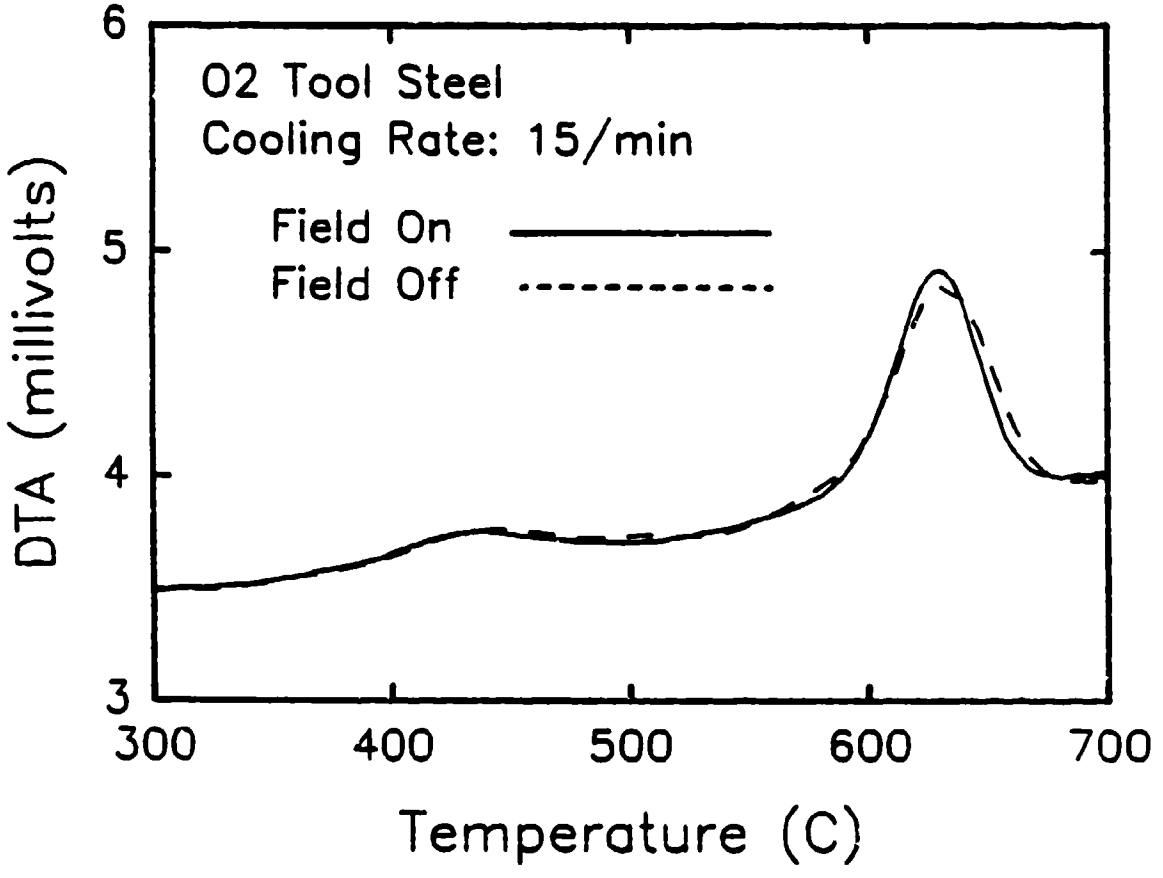

Figure 7. DTA output for continuous cooling of O_2 tool steel at an average rate of 50°C/min for E-field-on and E-field-off conditions. The two peaks reflect a roughly equal mix of pearlite and bainite.

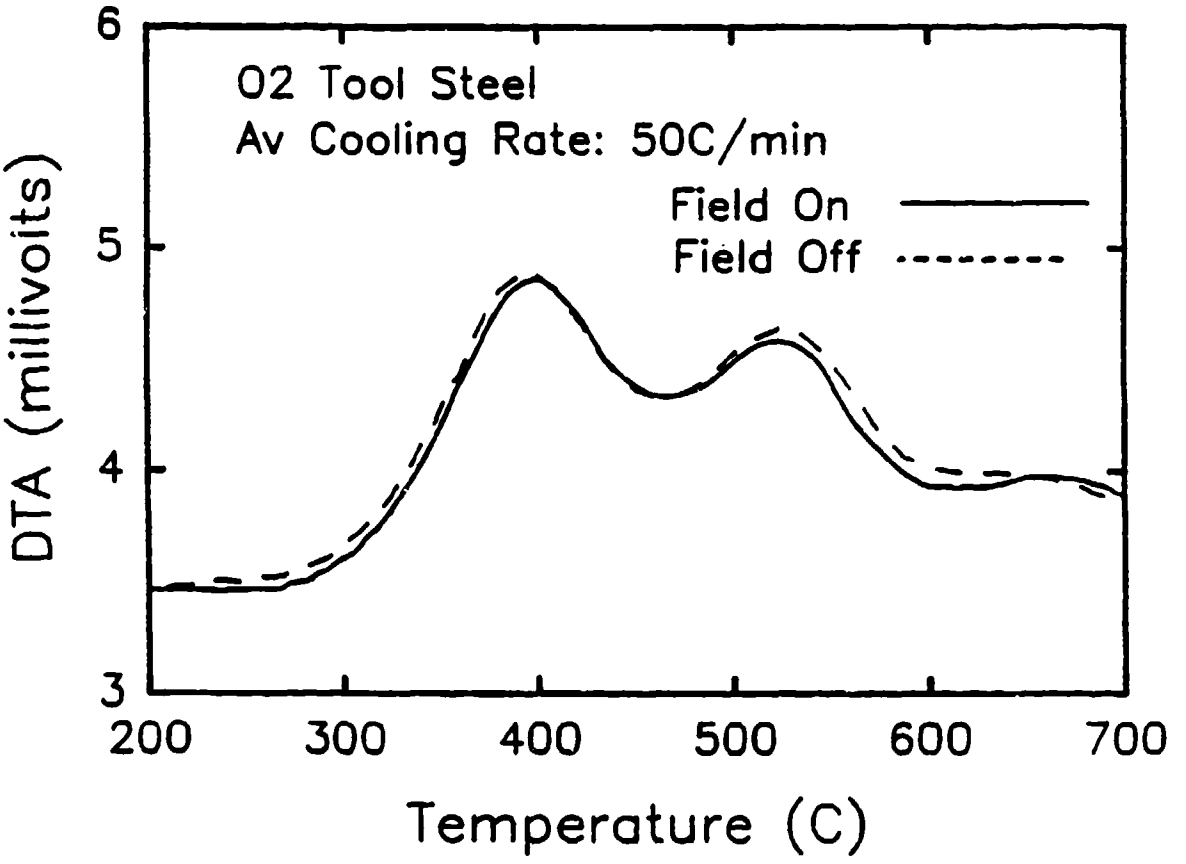

Figure 8. DTA output for continuous cooling of O_2 tool steel at a rate of 15°C/min for E-field-on and E-field-off conditions. Only a vestige of the bainite peak remains at this slow cooling rate indicating the preponderance of pearlite in the microstructure.

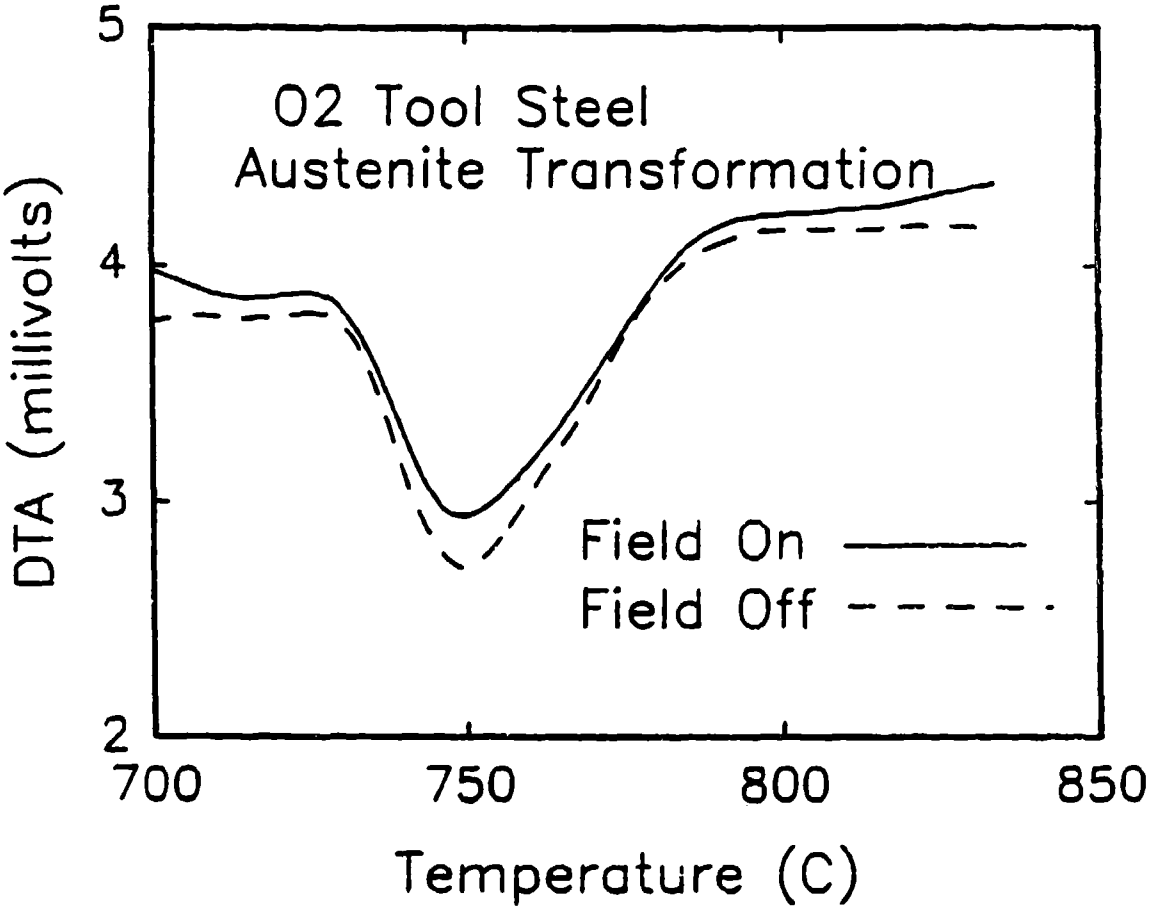

Figure 9. DTA output for the formation of austenite on heating O_2 tool steel at 25°C/min under E-field-on (3 kV/cm) and E-field-off conditions.

TECHNICAL REPORT INTERNAL DISTRIBUTION LIST

	NO. OF COPIES
CHIEF, DEVELOPMENT ENGINEERING DIVISION	
ATTN: SMCAR-CCB-D	1
-DA	1
-DC	1
-DI	1
-DP	1
-DR	1
-DS (SYSTEMS)	1
CHIEF, ENGINEERING SUPPORT DIVISION	
ATTN: SMCAR-CCB-S	1
-SE	1
CHIEF, RESEARCH DIVISION	
ATTN: SMCAR-CCB-R	2
-RA	1
-RE	1
-RM	1
-RP	1
-RT	1
TECHNICAL LIBRARY	5
ATTN: SMCAR-CCB-TL	
TECHNICAL PUBLICATIONS & EDITING SECTION	3
ATTN: SMCAR-CCB-TL	
OPERATIONS DIRECTORATE	1
ATTN: SMCWV-ODP-P	
DIRECTOR, PROCUREMENT DIRECTORATE	1
ATTN: SMCWV-PP	
DIRECTOR, PRODUCT ASSURANCE DIRECTORATE	1
ATTN: SMCWV-QA	

NOTE: PLEASE NOTIFY DIRECTOR, BENET LABORATORIES, ATTN: SMCAR-CCB-TL, OF ANY ADDRESS CHANGES.

TECHNICAL REPORT EXTERNAL DISTRIBUTION LIST

	NO. OF COPIES
ASST SEC OF THE ARMY RESEARCH AND DEVELOPMENT ATTN: DEPT FOR SCI AND TECH THE PENTAGON WASHINGTON, D.C. 20310-0103	1
ADMINISTRATOR DEFENSE TECHNICAL INFO CENTER ATTN: DTIC-FDAC CAMERON STATION ALEXANDRIA, VA 22304-6145	12
COMMANDER US ARMY ARDEC ATTN: SMCAR-AEE	1
SMCAR-AES, BLDG. 321	1
SMCAR-AET-O, BLDG. 351N	1
SMCAR-CC	1
SMCAR-CCP-A	1
SMCAR-FSA	1
SMCAR-FSM-E	1
SMCAR-FSS-D, BLDG. 94	1
SMCAR-IMI-I (STINFO) BLDG. 59 PICATINNY ARSENAL, NJ 07806-5000	2
DIRECTOR US ARMY BALLISTIC RESEARCH LABORATORY ATTN: SLCBR-DD-T, BLDG. 305 ABERDEEN PROVING GROUND, MD 21005-5066	1
DIRECTOR US ARMY MATERIEL SYSTEMS ANALYSIS ACTV ATTN: AMXSY-MP ABERDEEN PROVING GROUND, MD 21005-5071	1
COMMANDER HQ, AMCCOM ATTN: AMSMC-IMP-L ROCK ISLAND, IL 61299-6000	1
COMMANDER ROCK ISLAND ARSENAL ATTN: SMCRI-ENM ROCK ISLAND, IL 61299-5000	1
DIRECTOR US ARMY INDUSTRIAL BASE ENGR ACTV ATTN: AMXIB-P ROCK ISLAND, IL 61299-7260	1
COMMANDER US ARMY TANK-AUTMV R&D COMMAND ATTN: AMSTA-DDL (TECH LIB) WARREN, MI 48397-5000	1
COMMANDER US MILITARY ACADEMY ATTN: DEPARTMENT OF MECHANICS WEST POINT, NY 10996-1792	1
US ARMY MISSILE COMMAND REDSTONE SCIENTIFIC INFO CTR ATTN: DOCUMENTS SECT, BLDG. 4484 REDSTONE ARSENAL, AL 35898-5241	2
COMMANDER US ARMY FGN SCIENCE AND TECH CTR ATTN: DRXST-SD 220 7TH STREET, N.E. CHARLOTTESVILLE, VA 22901	1
COMMANDER US ARMY LABCOM MATERIALS TECHNOLOGY LAB ATTN: SLCMT-IML (TECH LIB) WATERTOWN, MA 02172-0001	2

NOTE: PLEASE NOTIFY COMMANDER, ARMAMENT RESEARCH, DEVELOPMENT, AND ENGINEERING CENTER, US ARMY AMCCOM, ATTN: BENET LABORATORIES, SMCAR-CCB-TL, WATERVLIET, NY 12189-4050, OF ANY ADDRESS CHANGES.

TECHNICAL REPORT EXTERNAL DISTRIBUTION LIST (CONT'D)

	NO. OF COPIES
COMMANDER US ARMY LABCOM, ISA ATTN: SLCIS-IM-TL 2800 POWDER MILL ROAD ADELPHI, MD 20783-1145	1
COMMANDER US ARMY RESEARCH OFFICE ATTN: CHIEF, IPO P.O. BOX 12211 RESEARCH TRIANGLE PARK, NC 27709-2211	1
DIRECTOR US NAVAL RESEARCH LAB ATTN: MATERIALS SCI & TECH DIVISION CODE 26-27 (DOC LIB) WASHINGTON, D.C. 20375	1 1
DIRECTOR US ARMY BALLISTIC RESEARCH LABORATORY ATTN: SLCBR-IB-M (DR. BRUCE BURNS) ABERDEEN PROVING GROUND, MD 21005-5066	1
COMMANDER AIR FORCE ARMAMENT LABORATORY ATTN: AFATL/MN EGLIN AFB, FL 32542-5434	1
COMMANDER AIR FORCE ARMAMENT LABORATORY ATTN: AFATL/MNF EGLIN AFB, FL 32542-5434	1
MIAC/CINDAS PURDUE UNIVERSITY 2595 YEAGER ROAD WEST LAFAYETTE, IN 47905	1

NOTE: PLEASE NOTIFY COMMANDER, ARMAMENT RESEARCH, DEVELOPMENT, AND ENGINEERING CENTER, US ARMY AMCCOM, ATTN: BENET LABORATORIES, SMCAR-CCB-TL, WATERVLIET, NY 12189-4050, OF ANY ADDRESS CHANGES.

END

FILMED

DATE: 12-91

DTIC